NUMERICAL STUDY ON LAMINAR NON-PREMIXED COMBUSTION OF N-HEPTANE AND AIR

ZHANG Xin, LI Jun-wei, ZHOU Zhao-qiu, YANG Fei, WANG Ning-fei

Email：zhangxin8707@gmail.com

(School of Aerospace Engineering, Beijing Institute of Technology, Beijing 100081, China)

Abstract

Combined with the detailed gas phase reaction mechanism, a 2D numerical simulation on the laminar non-premixed combustion of n-heptane and air inside a micro-tube is undertaken to investigate the effects of equivalence ratio of the mixture, inlet gas velocity, heat loss at the wall and size of the combustion chamber, using the modified creslaf model of CHEMKIN. The results show that, when equivalence ratio is set to 1.2, completely non-premixed combustion is happened. The highest temperature is obtained when equivalence ratio is set to 0.3, although where the flame is small and combustion is extremely incomplete. Inlet gas velocity strongly influences the combustion characteristics, such as combustion zone and flame plume length, while it has no effect on the flame temperature. Coefficient of heat transfer on chamber outer wall has a great impact on the wall temperature, while it has less effect on the flame core temperature. The results also could be seen that in the micro-combustion, the size of combustor has a big influence on the non-premixed combustion characteristics. The combustion trends to have some characteristics of premixed combustion when the size of combustor is reduced to a certain value in laminar flow model.

Keyword: micro-combustion, detailed reaction mechanism, non-premixed combustion, laminar flow, 2D numerical simulation

1. Introduction

With the recognitions of broad potential applications not only for electrical power but for heat and mechanical power sources, combustion at micro scale is collecting growing attentions these days [1-5]. One of the key factors for the success of micro-power systems is to realize sustainable and stable combustion in micro-scale combustors [6]. Now days in micro combustion research, premixed flames have typically been used and many fundamental studies have been conducted [7-10] while there is little research about the non-premixed combustion. Moreover, in most practical applications, in order to control fire safety and flame stability, fuel and oxidizer are injected separately into the combustion chamber and then mixed by turbulent flow [11], so it is important and necessary to study the detailed characteristics of non-premixed combustion.

Now days, researches about micro non-premixed combustion have aroused increasing attention [12-15]. While, reduced reaction mechanism is used in most of the numerical simulation of micro non-premixed combustion, that causes the simulated results can not accurately meet the experimental studies [16]. In this paper, combined with the detailed gas phase reaction mechanism, a 2D numerical simulation on the laminar non-premixed

combustion of n-heptane and air inside a micro-tube is undertaken to investigate the effects of equivalence ratio of the mixture, inlet gas velocity, heat loss at the wall and size of the combustion chamber.

2. Computational model

Modified creslaf model (cylindrical shear flow reactor model) [17] of CHEMKIN4.1 is used in this simulation study. By default, the creslaf model uses the uniform inlet and initial profile for all variables except axial velocity. The default inlet velocity profile is considered to be fully developed, i.e., parabolic. In this study, a co-annular flow inlet condition is established by using the user routine option (creslaf_user_routines.f) to override the default inlet profiles. A non-premixed flame is established downstream as fuel and air are mixed due to diffusion. The co-flowing annular jet configuration is shown in Fig.1 and properties of modified chamber model are given in Table 1.

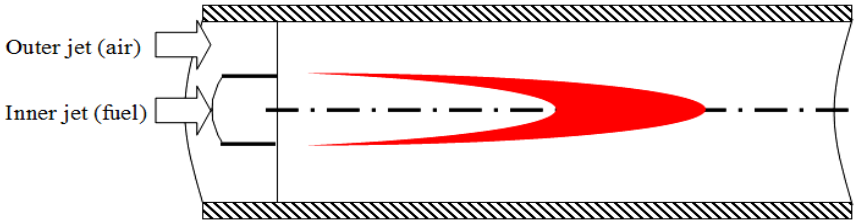

Figure 1. The co-flowing annular jet configuration

Non-adiabatic model is taken in this study in order to analysis the effects of heat loss. Grid is divided into axial 100×radial 40. Due to limitations on space, the following assumption are made： 1.steady laminar flow model; 2.no gas radiation; 3. no wall axial heat conduction; 4. convection (for species, mass, and energy) assumed to dominate in the axial direction, such that axial diffusion is neglected.

Table 1. Properties of modified chamber model

	Inner Jet	**Outer Jet**
Radius(mm)	$r = 0.3$	$R = 2$
Length(mm)	$l = 0$	$L = 50$
Initial Temperature[a] (K)	T_1=400	T_2=1400
C_7H_{16} Mass Fraction	1.0	0
O_2 Mass Fraction	0	0.21
N_2 Mass Fraction	0	0.79

[a] ambient temperature： 300K

2.1 Model equation

Nomenclature

a_e	Reactor surface area per unit length, cm	y	Cross-stream coordinate, cm
c_P	Specific heat at constant pressure of gas	$\dot{m}$	Mass flux, g/sec

	mixture, ergs/(g· K)	P	Pressure, dynes/cm^2
c_{Pk}	Specific heat capacity at constant pressure of the kth species	Q_e	Heat flux from outer wall to ambient environment, ergs(cm·sec)
D_{km}	Mixture-averaged diffusion coefficient of the kth species, cm^2/sec	R	Universal gas constant
g	Acceleration of gravity, cm/sec^2	T	Temperature, K
h_e	Heat transfer coefficient of outer wall, ergs/(sec K)	T_∞	Ambient temperature, K
h_k	Specific enthalpy of the kth species, ergs/g	u	Axial velocity of fluid mixture, cm/sec
K_g	Total number of gas-phase species	$V_{k,y}$	Diffusion velocity of the kth species in the y division, cm/sec
$\dot{m}_l$	Mass loss rate at the lower boundary, g/sec	Greeks	
$\dot{m}_u$	Mass loss rate at the upper boundary, g/sec	ρ	Mass density of a gas mixture, g/cm^3
$\bar{W}$	Mean molecular weight of a mixture, g/mole	ρ_i	Mass density at the reactor inlet, g/cm^3
W_k	Molecular weight of the kth species, g/mole	μ	Mixture viscosity, g/(cm·sec)
Y_k	Mass fraction of the kth species	ξ	Normalized stream function
x	Spatial coordinate along principal flow direction, cm	$\dot{\omega}_k$	Chemical production rate of the kth species due to gas-phase reactions, mole/(cm^3·sec)
		λ	Thermal conductivity of the gas mixture, ergs/cm·sec·K

Momentum：

$$\rho u\frac{\partial u}{\partial x}-\frac{\rho u}{\dot{m}}(\xi\frac{d\dot{m}}{dx}-\frac{d\dot{m}_l}{dx})\frac{\partial u}{\partial \xi}+\frac{dP}{dx}=\frac{\rho u}{\dot{m}^2}\frac{\partial}{\partial \xi}(\rho\cdot u\cdot\mu\cdot y^2\cdot\frac{\partial u}{\partial \xi})+g(\rho_i-\rho) \quad (1)$$

Species：

$$\rho u\frac{\partial Y_k}{\partial x}-\frac{\rho u}{\dot{m}}(\xi\frac{d\dot{m}}{dx}-\frac{d\dot{m}_l}{dx})\frac{\partial Y_k}{\partial \xi}=\dot{\omega}_k W_k-\frac{\rho u}{\dot{m}}\frac{\partial}{\partial \xi}(\rho y Y_k V_{k,y}) \qquad k=1,\ldots,K_g \quad (2)$$

Energy：

$$\rho u c_P\frac{\partial T}{\partial x}-\frac{\rho u c_P}{\dot{m}}(\xi\frac{d\dot{m}}{dx}-\frac{d\dot{m}_l}{dx})\frac{\partial T}{\partial \xi}=\frac{\rho u}{\dot{m}^2}\frac{\partial}{\partial \xi}(\rho u\lambda y^2\frac{\partial T}{\partial \xi})-\sum_{k=1}^{K_g}\dot{\omega}_k W_k h_k$$
$$-\frac{\rho^2 u y}{\dot{m}}\sum_{k=1}^{K_g}Y_k V_{k,y}c_{pk}\frac{\partial T}{\partial \xi} \quad (3)$$

State：

$$P=\frac{\rho RT}{\bar{W}} \quad (4)$$

Multicomponent transport is used, and diffusion velocity is given by:

$$V_{k,y}=\frac{D_{km}\rho u y}{X_k\dot{m}}\frac{\partial X_k}{\partial \xi}-\frac{D_k^T}{\rho Y_k}\frac{\rho u y}{T\dot{m}}\frac{\partial T}{\partial \xi} \quad (5)$$

In creslaf model, normalized stream function ξ is the independent variable instead of cross-stream coordinator y to simplify the model structure and improve efficiency in creslaf model, steam function is defined by：

Stream function：

$$\psi = \frac{1}{2}\int_0^y \rho u dy^2 \tag{6}$$

Normalized stream function：

$$\xi = \frac{\psi}{\dot{m}} \tag{7}$$

The relationships between the physical coordinates (y, x) and the transformed coordinates (ξ, ψ, x) are stated in the following equations that define the Von Mises Transformation [18]

$$(\frac{\partial}{\partial x})_y = (\frac{\partial}{\partial x})_\psi - \rho u y(\frac{\partial}{\partial \psi})_x + \frac{d\dot{m}_l}{dx}(\frac{\partial}{\partial \psi})_x \tag{8}$$

$$(\frac{\partial}{\partial x})_y = [(\frac{\partial}{\partial x})_\xi - (\frac{\xi}{\dot{m}}\frac{d\dot{m}}{dx} - \frac{1}{\dot{m}}\frac{d\dot{m}_l}{dx})(\frac{\partial}{\partial \xi})_x] - \rho v y^a \frac{1}{\dot{m}}(\frac{\partial}{\partial \xi})_x \tag{9}$$

$$(\frac{\partial}{\partial y})_x = \rho u y^a (\frac{\partial}{\partial \psi})_x = \rho u y^a (\frac{\partial}{\partial \xi})_x \tag{10}$$

2.2 Boundary conditions

1. uniform profiles are used for gas initial velocity u, initial temperature T in chamber inlet;2.chamber outlet pressure is standard atmosphere pressure P_∞； 3.no-slip wall model is used, that's meaning, in inner surface of chamber, $u = 0$, $V_{k,y} = 0$；4.without considering the effects of wall thickness, heat transfer between wall and ambient environment is defined by：

$$Q_e = a_e h_e (T_\infty - T) \tag{11}$$

2.3 Reaction mechanism

The reaction mechanism for n-heptane was obtained from the Lawrence Livermore National Laboratory n-heptane mechanism version 38 (dated 2000), which made up of 770 reversible elementary reactions among 175 species. Detailed chemical kinetic mechanism has been developed and used to study the oxidation of n-heptane in flow reactors, shock tubes and rapid compression machines, results show that the mechanism can maintain accuracy and efficiency in wide initial conditions range [19].

3. Results and discussion

3.1 Effects of fuel-air equivalence ratio

Fuel-air equivalence ratio is an important parameter that influences the non-premixed combustion characteristics. In order to analysis the influences of fuel-air equivalence ratio on the combustion, numerical computation is performed for inlet gas velocity of 700cm/s and heat transfer coefficient of chamber outer wall of 20W/m^{2}K over a wide range of fuel-air equivalence ratio. 2D chamber temperature distribution of different fuel-air equivalence ratio is showed in Fig.2. It can be seen that, the non-premixed flame is small when fuel-air

equivalence ratio is 0.3, and flame progressively become larger with the increase of fuel-air equivalence ratio. From Fig.2, we also can see that, when equivalence ratio increased to 3.0, non-premixed flame is divided into two parties by the initial flow of n-heptane. The reason of it is because the equivalence ratio equals to 3.0 means n-heptane is much excessive than that of the stoichiometric combustion, non-premixed combustion can't be happened at center of chamber entrance where is fuel-rich/air-lean conditions. The simulation results show that, with equivalence ratio increases, the peak flame temperature slightly lower. Peak flame temperature of equivalence ratio of 0.3 is highest, that is 2602K at 5.5mm from the entrance of chamber, which is different from characteristics of premixed combustion.

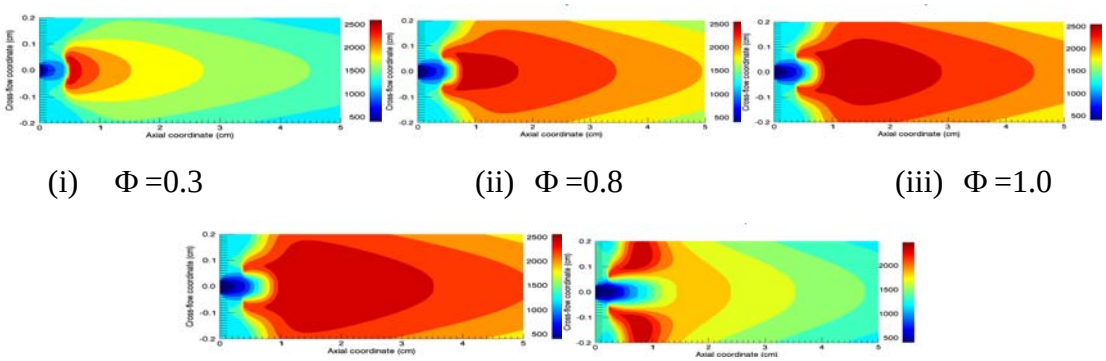

(i) Φ =0.3 (ii) Φ =0.8 (iii) Φ =1.0

(iv) Φ =1.2 (v) Φ =3.0

Figure 2. Chamber temperature with different fuel-air equivalence ratio

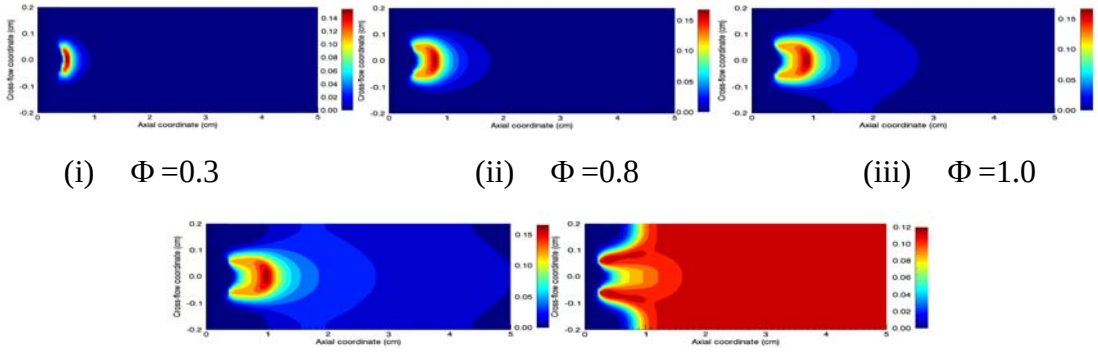

(i) Φ =0.3 (ii) Φ =0.8 (iii) Φ =1.0

(iv) Φ =1.2 (v) Φ =3.0

Figure 3. CO concentration distribution with different fuel-air equivalence ratio

Influence of equivalence ratio on CO concentration distribution is depicted in Fig.3. It can be seen from Fig.3 (a) that distribution area of CO expands gradually with increases of equivalence ratio. It obviously can be seen that, when equivalence ratio increases to 3.0, CO almost covers entire region of chamber behind the combustion.

In simulation, laminar flow model and no-slip wall model are used, so changes of gas velocity at center line of chamber would more accurately reflect the changes of gas velocity at chamber. From Fig.4 we can see that, the axial velocity increases sharply in the combustion zone. In the combustion zone, the huge amount of the heat produced by the combustion is released in a very small distance and thus causes the sharp increases of gas velocity. While, after combustion is finished and due to the strong heat transfer to the gas and wall, velocity

decreases along the flow direction. Under the same total inlet gas velocity, the larger gas axial velocity in the chamber means the more heat produced by the combustion. From Fig.4 it can be seen that, the peak value of gas velocity is largest (1833cm/s) when equivalence ratio is 1.2, which means that non-premixed combustion is most completely at this time. While when equivalence ratio is 0.3 and 3.0, the peak value of gas velocity is lower indicating that the combustion is not sufficient due to the conditions of fuel-rich or fuel-lean.

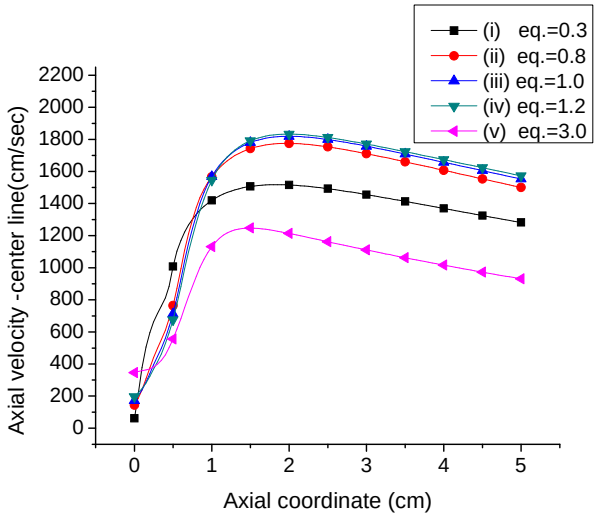

Figure 4. Axial velocity at center line of chamber with different fuel-air equivalence ratio

3.2 Effects of the inlet gas velocity

Inlet gas velocity has a big influence on the characteristics of non-premixed combustion, which directly effects the mixing between reactants as well as reactant and combustion products. In order to analysis the influences of the inlet gas velocity on the combustion, numerical computation is performed for equivalence ratio of 1.0 and heat transfer coefficient of chamber outer wall of $20W/m^2K$ over a wide range of inlet gas velocity. The effects of inlet gas velocity on temperature of chamber center line are shown in Fig.5, from figure we can see that, inlet gas velocity strongly influences the combustion characteristics, such as combustion zone and flame plume length, while it hardly effects on the peak flame temperature. As the velocity increases, the main reaction zone shifts downstream and flame plume become longer gradually. Fig.6 shows the temperature distribution in chamber when inlet gas velocity is 1325cm/s, it can be obviously seen that at this time part of the flame has run out of the chamber because of the large inlet gas velocity. The influences of the inlet gas velocity on the mole concentration of CO and CO_2 at the center line of chamber are shown in Fig.7. The same result is also demonstrated that as inlet gas velocity increases, the location of the peak value of CO and CO_2 mole concentration shifts downstream while the peak value of it almost no changes.

Under laminar flow model, the smaller inlet gas velocity means the residence time of the gas mixture in chamber is longer and gas mixture are easier to mix and ignite. As well as, the small inlet gas velocity equals to the small initial mass rate of gas mixture, thus during combustion there is no sufficient reactants to provided, non-premixed combustion don't maintain for a long time causing the shorter flame plume. In the same way, when inlet gas velocity increases, the contrary is the case.

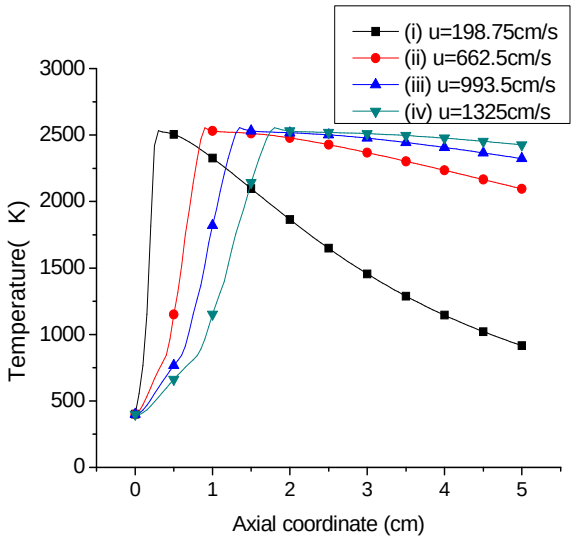

Figure 5. Temperature at center line of chamber with different inlet gas velocity

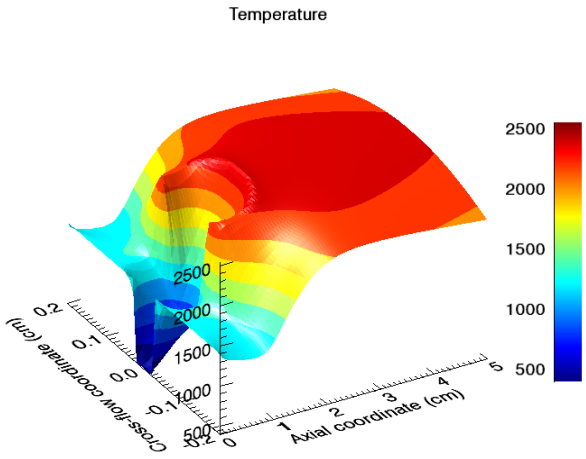

Figure 6. Temperature distribution in chamber when inlet gas velocity is 1325cm/s

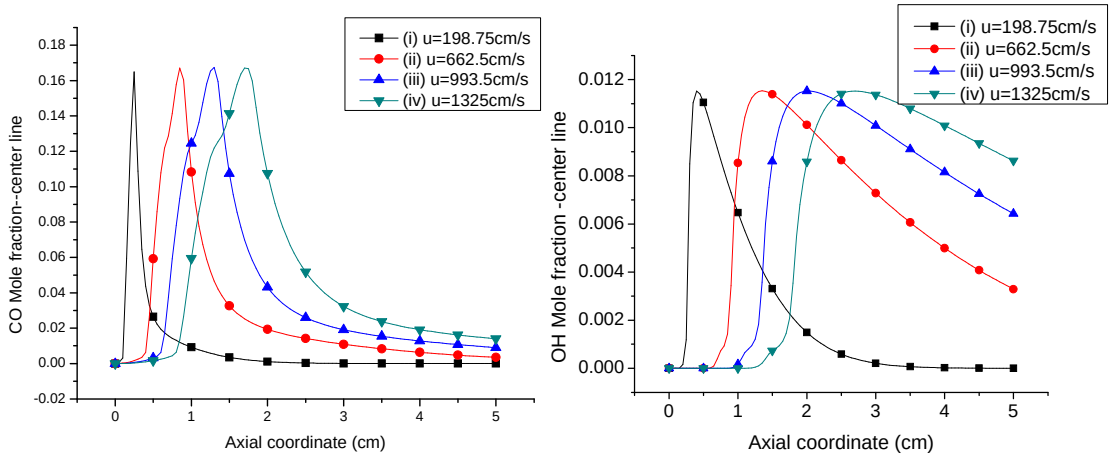

(a) CO mole concentration (b) CO_2 mole concentration

Figure 7. CO and CO_2 mole concentration at center line of chamber with different inlet gas velocity

3.3 Effects of the heat loss

In micro combustion, heat loss becomes one of the main factors affecting the combustion stability. In order to analysis the influences of the heat loss on the characteristics of the combustion, in this section, numerical simulation on four combustion models with different heat transfer coefficient of combustor outer wall(0、20W/m^{2}K、40W/m^2 K and 58W/m^{2}K) is undertaken with fuel-air equivalence ratio sets to 1.0 and inlet gas velocity is 530cm/s.

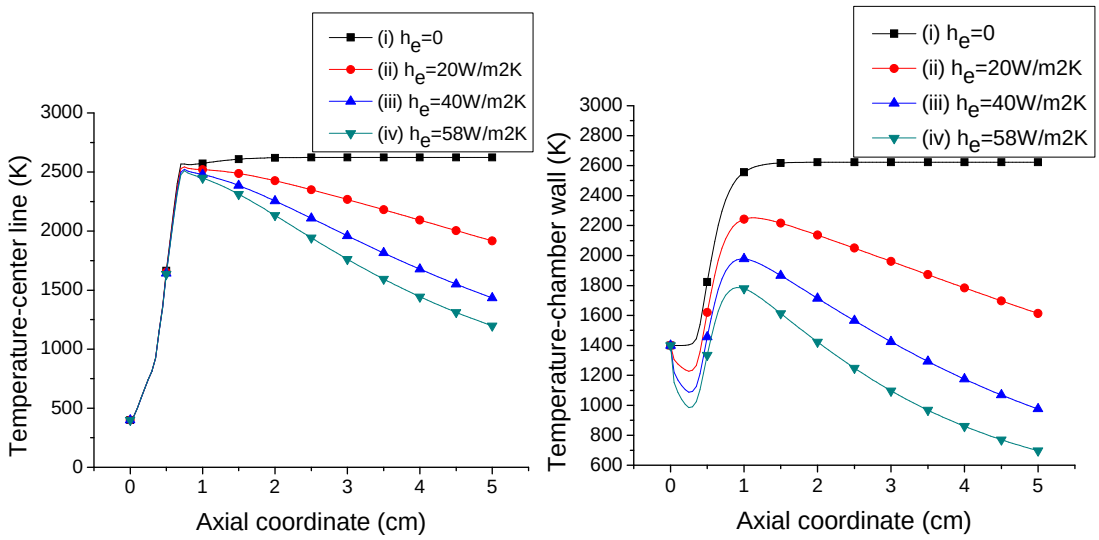

(a) temperature distribution at center line of chamber (b) surface temperature distribution at outer wall of chamber

Figure 8. Temperature distribution with different heat transfer coefficient of chamber outer wall

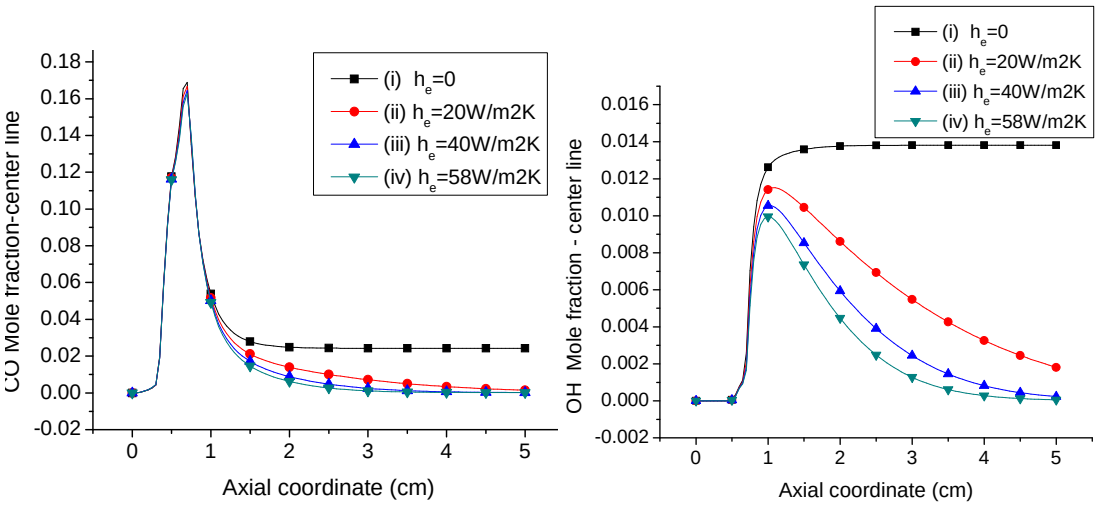

(a) CO mole concentration (b) OH mole concentration

Figure 9. CO and OH mole concentration at center line of chamber with different heat transfer coefficient of chamber outer wall

Simulation results show that, the non-premixed flame becomes the smaller with increases of heat transfer coefficient of chamber outer wall, and 58 W/m^{2}K is the upper flammable limit. Fig.8 shows the effects of heat transfer coefficient of chamber outer wall on the chamber temperature. From Fig.8 (a) we can see that heat transfer coefficient of chamber outer wall

has fewer influences on the location of flame ignition and peak flame temperature. While the decreasing rate of flame temperature after the combustion zone becomes larger gradually with the increases of the heat transfer coefficient of chamber outer wall. From Fig.8 (b), surface temperature distribution of chamber outer wall is complex. For example, outer wall temperature decreases from inlet temperature 1400K to 1227K at 2.5mm away from chamber entrance when heat transfer coefficient of chamber outer wall is 20 W/m^2K under the influences of gas mixing and wall heat loss where the gas mixture having not to be ignited yet. Then gas mixture begins to burn and produces a lot of heats, flame temperature reach to the maximum 2251K at 11mm away from chamber entrance. Behind the combustion zone, the temperature down again due to the heat loss and chamber outlet temperature downs to 1613K. The effects of heat transfer coefficient of chamber outer wall on the reaction intermediate products are shown in Fig.9, such as CO and OH. We can be seen that, heat transfer coefficient of chamber outer wall has dig influences on reaction mechanism. For instance, in adiabatic model, there are a larger number of intermediate products such as CO and OH in the exhaust of combustor.

3.4 Effects of combustor size

In micro combustion, as a result of the reduced size, the combustor surface-to-volume ratio increases (since this ratio scales as the inverse of the length scale). And high surface-to-volume ratio increases the relative heat losses that could quench the combustion process or reduce ignition reliability. In order to analysis the influences of the combustor size, numerical computation are performed for four combustor model when equivalence ratio is 1.0, inlet mass rate is 1.34×10^{-2}g/s and heat transfer coefficient of chamber outer wall sets to $20W/m^2K$. The parameters of four combustor model are summarized in Table 2.

Table 2. Parameters of different chamber model

	r (mm)	**R (mm)**	**L (mm)**
Model 1	0.6	4.0	50
Model 2	0.48	3.2	50
Model 3	0.36	2.4	50
Model 4	0.3	2.0	50

It is obvious in Fig.10 that the effects of the combustor size on the flame temperature and flame profile are very significant. From Fig.10 (a) we can see that, for model 1, non-premixed flame shows “mushroom” shape, and there are two distinct apophysises in the flame root near the combustor entrance. That’s because for model 1, the gas mixture inlet gas velocity is lowest comparing with other three models in the same total mass rate case, good mixing couldn’t be happened in the combustor entrance causing non-premixed combustion happens in boundary of fuel and air stream. As the combustor size decreases, the location of non-premixed flame shifts downstream and flame root become smooth. For model 4, the

combustor temperature distribution shows two discontinuous high temperature zone and combustion trends to have some characteristic of premixed combustion. The effects of combustor size on temperature distribution of centerline of combustor are shown in Fig.10 (b). We can see that, flame temperature increases sharply in the combustion zone; combustor size hardly affects the peak flame temperature and the location of the peak flame temperature shifts downstream gradually with the combustor size decreases.

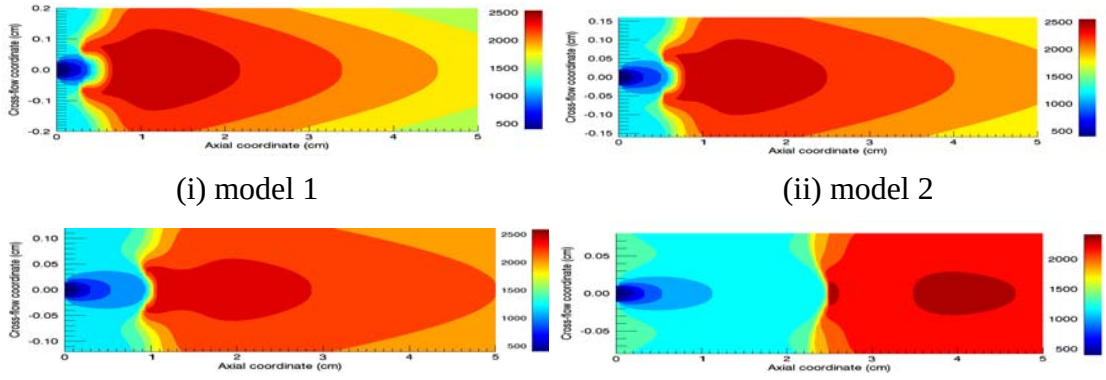

(i) model 1 (ii) model 2

(iii) model 3 (iv) model 4

(a) 2D distribution of temperature with different chamber size

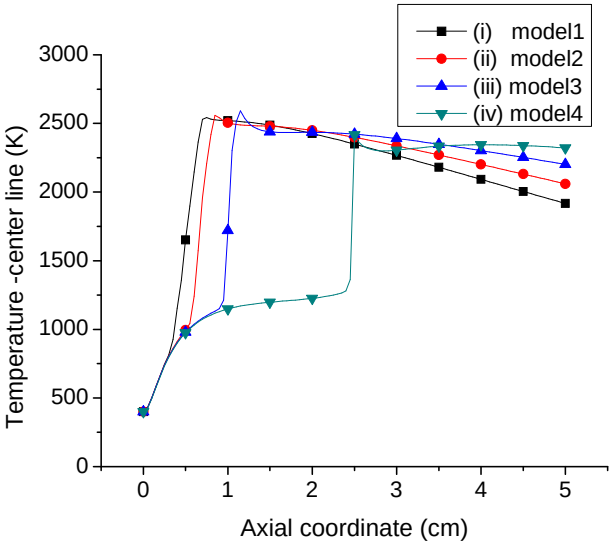

(b) Temperature distribution of center line of chamber with different chamber size

Figure 10. Chamber temperature distribution with different combustor size

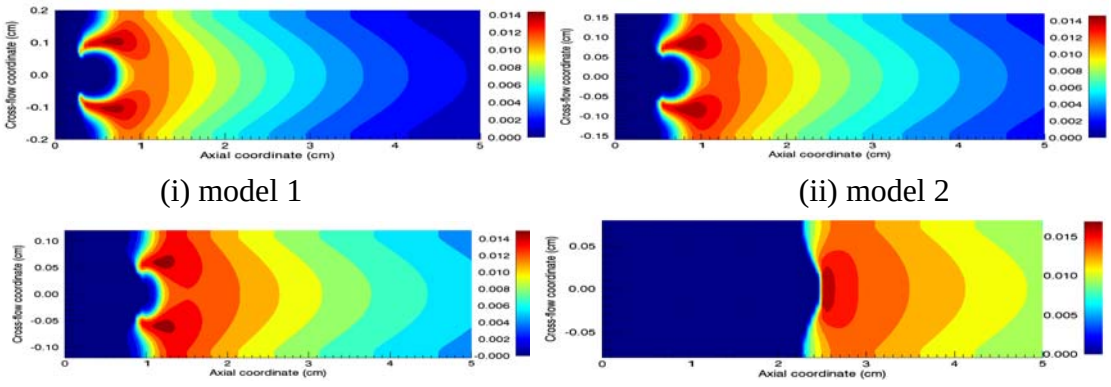

(i) model 1 (ii) model 2

(iii) model 3 (iv) model 4

Figure 11. Effects of combustor size on OH concentration distribution

Fig.11 shows the effects of combustor size on OH concentration distribution. It can be seen that, in model 1, great amount OH are produced in two obvious apophysises in the front of combustion zone. As combustor size decreases, the two apophysises become smaller. In model 4, two apophysises disappears and the location of peak value of OH concentration shifts to the centerline of combustor indicating again that the flame trends to have some characteristic of premixed combustion when the size of combustor is reduced to a certain value in laminar flow model.

4. Conclusion

In summary, a numerical simulation on the laminar non-premixed combustion of n-heptane and air inside a micro-tube was undertaken Combined with the detailed gas phase reaction mechanism. The effects of equivalence ratio of the mixture, inlet gas velocity, heat loss at the wall and size of the combustor are discussed in this paper. Results show that：

1. Fuel-air equivalence ratio has a big influence on the characteristics of non-premixed combustion; completely non-premixed combustion is happened when equivalence ratio is 1.2, and the smaller the equivalence ratio, the higher the peak flame temperature within flammable range.
2. Inlet gas velocity strongly influences the combustion characteristic, such as combustion zone and flame plume length, while it has no effect on the flame temperature.
3. Heat transfer coefficient of chamber outer wall has a great impact on the wall temperature, while it has fewer influences on the flame core temperature. The simulation results show that, upper flammable limit of the heat transfer coefficient of combustor outer wall is 58 W/m^2K.
4. In the micro-combustion, the combustor size has a big influence on the non-premixed combustion characteristics. The flame trends to have some characteristics of premixed flame when the size of combustor is reduced to a certain value in laminar flow model and at this time the combustor temperature distribution shows two discontinuous high temperature zones.

Acknowledgements

This research was supported by National Natural Science Foundation of China Nos. 50906004 and Doctoral Fund of Ministry of Education of China Nos. 200800071020.

References

[1] Hua Jinsong, Wu Meng, Kurichi K. Numerical simulation of the combustion of hydrogen-air mixture in micro-scaled chambers (I): Fundamental study. Chemical Engineering Science, 2005, 60 (13): 3497-3506

[2] Hua Jinsong, Wu Meng, Kurichi K. Numerical simulation of the combustion of hydrogen-air mixture in micro-scaled chambers (II): CFD analysis for a micro-combustor. Chemical Engineering Science, 2005, 60 (13): 3507-3515

[3] Zhong Beijing, Wu Heng. Numerical simulation on catalytic combustion of CH4/air in micro-channel. Journal of Combustion Science and Technology, 2005 (2): 1-5

[4] D.G. Norton, D.G. Vlachos, A CFD study of propane/air micro-flame stability, Combustion and Flame 138 (2004) 97–107.
[5] Carlos Fernandez-Pello A. Micro-power generation using combustion: issues and approaches [C]. Twenty-Ninth International Symposium on Combustion. Sapporo, Japan, the Combustion Institute, 2002: 1 - 45.
[6] Fernandez-pello AC. Micro power generation using combustion: Issues and approaches [A]. Proceedings of the Combustion Institute. Sapporo, Japan, 2002. 883-899.
[7] Kim, N.I., Kataoka, T., Maruta, K., Maruyama, S. Flammability limits of stationary flames in tubes at low pressure. Combust. Flame 141, 78 – 88.
[8] Kim, N.I., Maruta, K. A numerical study on propagation of premixed flame in small tubes [J]. Combust. Flame 146, 283 – 301.
[9] Kim, N.I., Aizumi, S., Yokomori, T., Kato, S., Fujimori, T., Maruta, K. Development and scale effects of small swiss-roll combustors [J]. Proc. Combust. Inst. 31, 3243 – 3250.
[10] Kim, N.I. Effect of an inlet-temperature disturbance on the propagation of methane – air premixed flame in small tubes. Combust. Flame 156, 1332 – 1338.
[11] Bo Xu, Yiguang Ju. Studies on non-premixed flame streets in a meso-scale channel [J]. Proceedings of the Combustion Institute 32 (2009) 1375–1382
[12] Miesse, C., Masel, R., Short, M., Shannon, M.A. Diffusion flame instabilities in a 0.75 mm non-premixed micro burner [J]. Proc. Combust. Inst. 30, 2499 – 2507.
[13] Sinha, A., Ganguly, R., Puri, I.K. Control of confined non-premixed flames using a micro-jet [J]. Int. J. Heat Fluid Flow 26, 431 – 439.
[14] Xu, B., Ju, Y.G., 2009. Studies on non-premixed flame streets in a meso-scale channel [J]. Proc. Combust. Inst. 32, 1377 – 1382.
[15] Nam Il Kim *, Young Min Yun, Min Jung Lee. Non-premixed flame characteristics of opposed methane jets in coaxial narrow air stream tubes [J]. International Journal of Heat and Fluid Flow 31 (2010) 680 – 688
[16] JIANG Liqiao, ZHAO Daiqing, WANG Xiaohan. Structure and extinction characteristics of methane micro-diffusion flames [J]. 2007,13(2) : 183-186
[17] Reaction Design, Inc., CHEMKIN Release 4.1, San Diego, CA, 2006.
[18] F. K. Moore, High Speed Aerodynamics and Jet Propulsion (Princeton University Press, Princeton, NJ, 1964) , Vol. IV.
[19] Seiser. H, H. Pitsch, K. Seshadri, W. J. Pitz and H. J. Curran. Extinction and Autoignition of n-Heptane in Counter flow Configuration, Proceedings of the Combustion Institute, 2000, 28: 2029-2037.